Vessels delineation in retinal images using COSFIRE filters

George Azzopardi[1], Nicola Strisciuglio[1,2], Mario Vento[2], Nicolai Petkov[1]
[1]Johann Bernoulli Institute for Mathematics and Computer Science, University of Groningen
[2]Dept. of Information and Electrical Eng. and Applied Mathematics, University of Salerno - Italy
{g.azzopardi, n.strisciuglio, n.petkov}@rug.nl, mvento@unisa.it

Abstract

Retinal image analysis is widely used in the medical community to diagnose several pathologies. The automatic analysis of such images is important to perform more efficient diagnosis. We propose an effective method for the delineation of blood vessels in retinal images using trainable bar-selective COSFIRE filters. The results that we achieve on three publicly available data sets (DRIVE: Se = 0.7655*, Sp* = 0.9704*; STARE: Se* = 0.7763*, Sp* = 0.9695*; CHASE_DB1: Se* = 0.7699*, Sp* = 0.9476*) demonstrate the effectiveness of the proposed approach.*

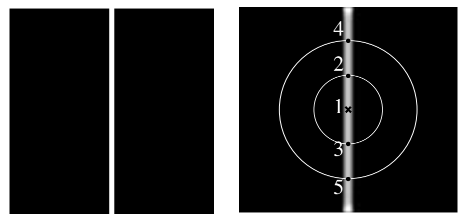

(a) (b)

Figure 1: Configuration of a COSFIRE filter (b) using a synthetic bar (a). The cross marker (labelled by '1') is the center of support of the filter while the enumerated spots represent the positions at which the strongest DoG responses are achieved.

1. Introduction

The retinal fundus photography is a non-invasive technique that is widely used by medical doctors to diagnose several pathologies. The automatic analysis of retinal images is important to facilitate the work required by medical doctors to diagnose such pathologies.

The delineation of blood vessels is a basic step of the automatic analysis of retinal fundus images. The methods proposed so far can be divided into two categories: unsupervised [1, 5, 7] and supervised [4, 6, 10, 11] approaches.

We propose a trainable bar-selective filter based on Combination of Receptive Fields (CORF) computational model of a simple cell in visual cortex [2] and its implementation called Combination of Shifted Filter Responses (COSFIRE) [3]. We demonstrate that it is highly tolerant to rotation and noise.

2. Proposed method

The proposed COSFIRE filter takes as input the responses of a group of Difference-of-Gaussians (DoG) filters at certain positions with respect to the center of its area of support. The positions at which we take the responses are determined in an automatic configuration process that extracts information about a given synthetic bar pattern, Fig. 1a. We consider the DoG filter responses along a number (in general k) of concentric circles around the center point (labelled by '1' in Fig. 1b). The result of the configuration is a set $S = \{(\sigma_i, \rho_i, \phi_i) \mid i = 1, \ldots, n\}$ of 3−tuples, where σ_i represents the standard deviation of the DoG filters, while ρ_i and ϕ_i are the polar coordinates with respect to the center of support of the filter. The response of a COSFIRE filter is computed as the weighted geometric mean of the responses of the concerned DoG filters at the positions determined in the configuration step:

$$r_S(x, y) \stackrel{\text{def}}{=} \left(\prod_{i=1}^{|S|} \left(s_{\sigma_i,\rho_i,\phi_i}(x, y)\right)^{\omega_i} \right)^{1/\sum_{i=1}^{|S|} \omega_i} \tag{1}$$

where $s_{\sigma_i,\rho_i,\phi_i}(x, y)$ is the blurred response of the i-th DoG filter weighted with a Gaussian function whose standard deviation $\sigma' = \sigma'_0 + \alpha\rho_i$ is a linear function of the distance ρ_i from the support center of the filter.

We manipulate the parameter ϕ_i, to obtain a new set $R_\psi(S) = \{(\sigma_i, \rho_i, \phi_i + \psi) \mid i = 1, \ldots, n\}$ with orientation preference ψ. Then, we consider the responses of COSFIRE filters with different orientation preferences by taking the maximum value at every location (x, y):

$$\hat{r}_S(x, y) \stackrel{\text{def}}{=} \max_{\psi \in \Psi} \left\{ r_{R_\psi(S)}(x, y) \right\} \tag{2}$$

where $\Psi = \{0, \frac{\pi}{12}, \frac{\pi}{6}, \ldots, \frac{11\pi}{12}\}$.

		DRIVE				STARE				CHASE_DB1			
	Method	**Se**	**Sp**	**AUC**	**Acc**	**Se**	**Sp**	**AUC**	**Acc**	**Se**	**Sp**	**AUC**	**Acc**
Unsup.	**COSFIRE**	**0.7655**	**0.9704**	**0.9614**	**0.9442**	**0.7763**	**0.9695**	**0.9555**	**0.9496**	**0.7699**	**0.9476**	**0.9497**	**0.9305**
	Mendonca et al. [7]	0.7344	0.9764	-	0.9463	0.6996	0.9730	-	0.9479	-	-	-	-
	Al-Rawi et al. [1]	-	-	0.9435	0.9535	-	-	0.9467	0.9090	-	-	-	-
	Ricci and Perfetti [10]	-	-	0.9558	0.9563	-	-	0.9602	0.9584	-	-	-	-
Sup.	Staal et al. [12]	-	-	0.9520	0.9441	-	-	0.9614	0.9516	-	-	-	-
	Soares et al. [11]	0.7332	0.9782	0.9614	0.9466	0.7207	0.9747	0.9671	0.9480	-	-	-	-
	Ricci and Perfetti [10]	-	-	0.9633	0.9595	-	-	0.9680	0.9646	-	-	-	-
	Marin et al. [6]	0.7067	0.9801	0.9588	0.9452	0.6944	0.9819	0.9769	0.9526	-	-	-	-
	Fraz et al. [4]	0.7406	0.9807	0.9747	0.9480	0.7548	0.9763	0.9768	0.9534	0.7224	0.9711	0.9712	0.9469

Table 1: Performance results of COSFIRE operator on DRIVE, STARE and CHASE_DB1 data sets compared to other methods.

3. Results

We evaluated the method on three benchmark data sets, called DRIVE [12], STARE [5] and CHASE_DB1 [9] that are composed of 40, 20 and 28 images, respectively. These data sets come with ground truth images that have been considered as gold standard for the performance measurement.

We binarized the output of the COSFIRE operator by using a threshold value as a fraction of the maximum response. In this way, every pixel is classified either as *vessel* or *non-vessel*. For each threshold value we matched the resulting binary image with the ground truth image and computed the number of true positives, false positives, true negative and false negatives. Then, using these values we computed the Matthews Correlation Coefficient (MCC) as a performance measurements and chose the threshold that gave the maximum MCC average value over a given data set. For that threshold value we report the Accuracy (Acc), Sensitivity (Se) and Specificity (Sp). For comparison purpose, we computed the ROC curve and its underlying area (AUC). In Table 1 we report our results next to the ones published in the literature.

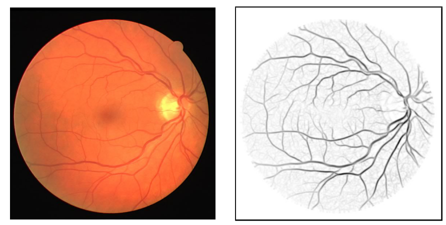

(a) (b)

Figure 2: (a) Input retinal image and (b) the (inverted) output of a rotation-invariant COSFIRE operator using 12 *orientation preferences.*

4. Conclusions

The results that we achieve on DRIVE, STARE and CHASE_DB1 data sets demonstrate the effectiveness of the proposed method. The COSFIRE filter is versatile as it can be automatically configured to detect any given vessel-like patterns, including bifurcations and crossovers.

The processing of a COSFIRE filter is very efficient. In fact, the proposed method is the most time-efficient algorithm for vessels delineation in retinal fundus images published so far.

References

[1] M. Al-Rawi, M. Qutaishat, and M. Arrar. An improved matched filter for blood vessel detection of digital retinal images. *Computer in biology and medicine*, 37(2):262–267, 2007.

[2] G. Azzopardi and N. Petkov. A CORF computational model of a simple cell that relies on LGN input outperforms the Gabor function model. *Biol Cybern*, 106(3):177–189, 2012.

[3] G. Azzopardi and N. Petkov. Trainable COSFIRE filters for keypoint detection and pattern recognition. *IEEE Trans Pattern Anal Mach Intell*, 35:490–503, 2013.

[4] M. Fraz, P. Remagnino, A. Hoppe, B. Uyyanonvara, A. Rudnicka, C. Owen, and S. Barman. An ensemble classification-based approach applied to retinal blood vessel segmentation. *IEEE Trans Biomed Eng*, 59(9):2538–2548, 2012.

[5] A. Hoover, V. Kouznetsova, and M. Goldbaum. Locating blood vessels in retinal images by piecewise threshold probing of a matched filter response. *IEEE Trans Med Imaging*, 19(3):203–210, 2000.

[6] D. Marin, A. Aquino, M. Emilio Gegundez-Arias, and J. Manuel Bravo. A New Supervised Method for Blood Vessel Segmentation in Retinal Images by Using Gray-Level and Moment Invariants-Based Features. *IEEE Trans Med Imaging*, 30(1):146–158, 2011.

[7] A. M. Mendonca and A. Campilho. Segmentation of retinal blood vessels by combining the detection of centerlines and morphological reconstruction. *IEEE Trans Med Imaging*, 25(9):1200–1213, 2006.

[8] M. Niemeijer, J. Staal, B. van Ginneken, M. Loog, and M. Abramoff. Comparative study of retinal vessel segmentation methods on a new publicly available database. In *Proc. of the SPIE - The International Society for Optical Engineering*, pages 648–56, 2004.

[9] C. G. Owen, A. R. Rudnicka, R. Mullen, S. A. Barman, D. Monekosso, P. H. Whincup, J. Ng, and C. Paterson. Measuring retinal vessel tortuosity in 10-year-old children: validation of the computer-assisted image analysis of the retina (caiar) program. *Invest Ophthalmol Vis Sci*, 50(5):2004–10, 2009.

[10] E. Ricci and R. Perfetti. Retinal blood vessel segmentation using line operators and support vector classification. *IEEE Trans Med Imaging*, 26(10):1357–1365, 2007.

[11] J. V. B. Soares, J. J. G. Leandro, R. M. Cesar, Jr., H. F. Jelinek, and M. J. Cree. Retinal vessel segmentation using the 2-D Gabor wavelet and supervised classification. *IEEE Trans Med Imaging*, 25(9):1214–1222, 2006.

[12] J. Staal, M. Abramoff, M. Niemeijer, M. Viergever, and B. van Ginneken. Ridge-based vessel segmentation in color images of the retina. *IEEE Trans Med Imaging*, 23(4):501–509, 2004.